Improved Sensorless Direct Torque and Flux Control of IPMSM based on On-line Parameter Estimation

M.X. Bui[1], D. Xiao[2] and M.F. Rahman[2]

[1] Faculty of Control Engineering, Le Quy Don Technical University, Vietnam
[2] School of Electrical Engineering and Telecommunications, University of New South Wales, Australia

***Abstract*-- This paper presents an improved direct torque and flux control of a sensorless control system with Interior Permanent Magnet Synchronous Motor (IPMSM). The estimation of torque and flux is enhanced by the real-time update of machine parameters including stator resistances, *d*- and *q*- axis inductance, permanent magnet flux linkage. The estimation of rotor speed and position is based on the measurement of current slopes at one zero- and two active-voltage vectors during every PWM cycle. The *d*- and *q*- axis inductances are estimated at PWM frequency based on those current derivatives and the DC bus voltage. The stator resistance and permanent magnet flux linkage which vary slowly due to temperature and aging factors are estimated based on the use of recursive least square technique. The numerical simulation and experimental study of the proposed methods show the effectiveness of the proposed parameter identification method and the improvement of estimated torque and flux of the sensorless control system.**

***Index Terms*— Direct torque and flux control, Sensorless control, IPMSM, Machine Parameter Identification, Current Derivative Measurement.**

I. INTRODUCTION

Permanent magnet synchronous motors (PMSM) have been applied widely in the industry due to high efficiency and high-power density. There are two main control schemes for PMSM including Field Oriented Control (FOC) and Direct Torque Control (DTC). The DTC brings faster control bandwidth of the torque control compared to FOC; however, DTC leads to higher current and torque ripples [1]. The Direct Torque and Flux Control can mitigate the current and torque ripple by introducing torque and flux controllers in addition to the space vector modulation technique [2].

Sensorless control which is the elimination of mechanical sensor, such as encoder, resolver have been developed significantly over recent decades. Sensorless methods helps to reduce the size and cost of the drive system. Especially, sensorless control also results in higher reliability of the drive system where the proper operation of mechanical sensors is affected by temperature range and vulnerable in the hostile working environment. The estimation of rotor speed and position can be based on the machine model [3, 4] or the injection of the test signals [5, 6]. The former methods are robust at medium and high speeds. However, at low and very low speed operations the low signal to noise and the non-linearity of the system affect significantly to the estimation accuracy of those methods. The approaches based on the injection of test signals and processing of the response are robust at low and very low speeds. However, these techniques result in high the current, torque ripple, and acoustic noise. The injected signal also limits the modulation index, hence the speed range. In addition, the bandwidth of the position and speed estimator is limited by the filters [7]. In order to overcome the weakness of the signal injection methods, the approaches utilize the fundamental pulse width modulation as the excitation have been developed. The slopes of phase current at voltage vectors during PWM cycles are used to estimate the rotor speed and position [8-10].

Direct torque and flux control scheme normally utilizes the nominal value of *d*- and *q*- axis inductances and permanent magnet flux linkage to estimate machine torque and flux as the feedback of their corresponding control loops. However, due to the saturation effect the machine inductances, especially the *q*- axis inductance varies significantly according to the variation of operating load current. In addition, due to the demagnetization the permanent magnet flux linkage varies after long running time. Consequently, the estimation of machine torque and flux using the nominal values suffers high deviation from the actual values. As a result, the dynamic performance of the control system deteriorates significantly. Therefore, there is a crucial need to identify these machine parameters fast and accurately and apply the estimated values to the torque and flux estimators.

So far, there have been a number of methods developed to identify machine parameters. These can be classified as off-line and on-line techniques. The off-line methods normally require the clamping system to lock the motor shaft [11] or a mover to rotate the rotor at the rated speed [12]. The weakness of the off-line methods is that it requires additional hardware for the test, takes time and effort to process a huge number of data. In addition, the variation of parameters due to aging factor and various operating states cannot be handled by these techniques. The on-line method based on the machine model and the application of recursive least square method, affine projection algorithm, model adaptive reference system can overcome the limits of the off-line methods [13-15]. However, these methods suffer the slow update of the estimated values due to the recursive nature of the algorithm, thus are unable to apply during fast transient operation. Furthermore, the injected signal of the methods for improvement of convergence capability results in the increase of current and torque ripple.

978-1-7281-5414-5/20/$31.00 ©2020 IEEE

Therefore, this paper proposes a new method to estimate machine parameters to improve the direct torque and flux control of the IPMSM control system. The *d*- and *q*-inductances are estimated very fast by measuring current derivatives at two active-voltage vectors and one-zero voltage vector during each PWM cycle. The stator resistance and permanent magnet flux linkage which varies slowly to the change of temperature and aging factor are identified by using the recursive least square approach. The current derivatives used to estimate machine inductances are also used to estimate rotor speed and position for sensorless control. Extensive numerical simulation and experimental studied have been conducted to verify the effectiveness of the proposed on-line parameter identification method and improvement of direct torque and flux control of the sensorless IPMSM control system.

II. Proposed Sensorless and On-line Parameters Estimation

A. Estimation of rotor speed and position

Dynamic model of IPMSM can be presented as:

$$V_S = R_S I_S + L_S \frac{dI_S}{dt} + E_S \tag{1}$$

where

$$V_S = \begin{bmatrix} V_a \\ V_b \\ V_c \end{bmatrix};\ I_S = \begin{bmatrix} i_a \\ i_b \\ i_c \end{bmatrix};\ L_S = \begin{bmatrix} L_{aa} & L_{ab} & L_{ac} \\ L_{ba} & L_{bb} & L_{bc} \\ L_{ca} & L_{cb} & L_{cc} \end{bmatrix};\ E_S = \begin{bmatrix} e_a \\ e_b \\ e_c \end{bmatrix}$$

where V_a, V_b, V_C are stator voltage of phase A, B and C; i_a, i_b, i_c are the stator current of phase A, B, and C; R_S, the stator resistance; e_A, e_B, e_C are the stator back EMF of phase A, B and C; L_{aa}, L_{bb}, L_{cc} are the stator self-inductance of phase A, B and C respectively; L_{ab}, L_{ba}, L_{ac}, L_{ca}, L_{bc}, L_{cb} are the mutual inductances between respective phases.
where

$$\begin{aligned}
L_{aa} &= L_\Sigma + L_\Delta \cos(2\theta_e) \\
L_{bb} &= L_\Sigma + L_\Delta \cos\left(2\theta_e + \frac{2\pi}{3}\right) \\
L_{cc} &= L_\Sigma + L_\Delta \cos\left(2\theta_e + \frac{4\pi}{3}\right) \\
L_{bc} &= L_{cb} = -\frac{L_\Sigma}{2} + L_\Delta \cos(2\theta_e) \\
L_{ab} &= L_{ba} = -\frac{L_\Sigma}{2} + L_\Delta \cos\left(2\theta_e - \frac{2\pi}{3}\right) \\
L_{ac} &= L_{ca} = -\frac{L_\Sigma}{2} + L_\Delta \cos\left(2\theta_e - \frac{4\pi}{3}\right)
\end{aligned} \tag{2}$$

where θ_e is the electrical angle of the rotor.

$$\begin{aligned}
L_\Sigma &= \frac{L_d + L_q}{3} \\
L_\Delta &= \frac{L_d - L_q}{3}
\end{aligned} \tag{3}$$

where L_d, L_q are direct- and quadrature- axes inductances respectively.

Assume that during every PWM the rotor angle is unchanged, the back EMFs of three phases remain constant and the voltage drop on stator resistance is negligible to DC bus voltage, the positional scalar p_a, p_b, p_c can be calculated as shown in Table I [9].

where

$$\begin{aligned}
p_A &= \frac{2L_\Delta}{L_\Sigma} cos(2\theta_e) \\
p_B &= \frac{2L_\Delta}{L_\Sigma} cos(2\theta_e - 2\pi/3) \\
p_C &= \frac{2L_\Delta}{L_\Sigma} cos(2\theta_e - 4\pi/3)
\end{aligned} \tag{4}$$

TABLE I
POSITION SCALARS OF IPMSM WITH STAR CONNECTION

Voltage vector	p_A	p_B	p_C
V_1, V_0	$2-g\left(\frac{di_A^{(1)}}{dt}-\frac{di_A^{(0)}}{dt}\right)$	$-1-g\left(\frac{di_C^{(1)}}{dt}-\frac{di_C^{(0)}}{dt}\right)$	$-1-g\left(\frac{di_B^{(1)}}{dt}-\frac{di_B^{(0)}}{dt}\right)$
V_2, V_0	$-1+g\left(\frac{di_B^{(2)}}{dt}-\frac{di_B^{(0)}}{dt}\right)$	$-1+g\left(\frac{di_A^{(2)}}{dt}-\frac{di_A^{(0)}}{dt}\right)$	$2+g\left(\frac{di_C^{(2)}}{dt}-\frac{di_C^{(0)}}{dt}\right)$
V_3, V_0	$-1-g\left(\frac{di_C^{(3)}}{dt}-\frac{di_C^{(0)}}{dt}\right)$	$2-g\left(\frac{di_B^{(3)}}{dt}-\frac{di_B^{(0)}}{dt}\right)$	$-1-g\left(\frac{di_A^{(3)}}{dt}-\frac{di_A^{(0)}}{dt}\right)$
V_4, V_0	$2+g\left(\frac{di_A^{(4)}}{dt}-\frac{di_A^{(0)}}{dt}\right)$	$-1+g\left(\frac{di_C^{(4)}}{dt}-\frac{di_C^{(0)}}{dt}\right)$	$-1+g\left(\frac{di_B^{(4)}}{dt}-\frac{di_B^{(0)}}{dt}\right)$
V_5, V_0	$-1-g\left(\frac{di_B^{(5)}}{dt}-\frac{di_B^{(0)}}{dt}\right)$	$-1-g\left(\frac{di_A^{(5)}}{dt}-\frac{di_A^{(0)}}{dt}\right)$	$2-g\left(\frac{di_C^{(5)}}{dt}-\frac{di_C^{(0)}}{dt}\right)$
V_6, V_0	$-1+g\left(\frac{di_C^{(6)}}{dt}-\frac{di_C^{(0)}}{dt}\right)$	$2+g\left(\frac{di_B^{(6)}}{dt}-\frac{di_B^{(0)}}{dt}\right)$	$-1+g\left(\frac{di_A^{(6)}}{dt}-\frac{di_A^{(0)}}{dt}\right)$

In Table I, the superscript 0÷6 indicates the voltage vector where current derivatives are measured to calculate the positional scalars; g is the quantity which is calculated based on measured current derivative as shown in Table II. The calculation of g is based on the assumption that during a PWM cycle the positional scalars are unchanged [9].

The positional scalar p_α and p_β on the stational reference frame can be calculated as:

$$\begin{aligned}
p_\alpha &= \frac{2p_A - p_B - p_C}{3} = \frac{2L_\Delta}{L_\Sigma} cos(2\theta_e) \\
p_\beta &= \frac{p_B - p_C}{\sqrt{3}} = -\frac{2L_\Delta}{L_\Sigma} sin(2\theta_e)
\end{aligned} \tag{4}$$

The phase lock loop is then applied to estimate the rotor speed and position [9].

B. Estimation of machine inductances

Quantity g shown in Table II can be also expressed as the function of DC bus voltage and the inductances in the stational reference frame as followed [16]:

$$g = \frac{9}{2V_{DC}} (L_\Sigma) \left(1 - \left(\frac{L_\Delta}{L_\Sigma}\right)^2\right) \tag{5}$$

From (4), the following equation can be derived:

$$\frac{L_\Delta}{L_\Sigma} = \frac{\sqrt{p_\alpha^2 + p_\beta^2}}{2} \tag{6}$$

Solving (5) and (6) yields the incremental inductances:

$$L_q = \frac{gV_{DC}}{3\left(1 - \frac{\sqrt{p_\alpha^2 + p_\beta^2}}{2}\right)}$$

$$L_d = \frac{gV_{DC}}{3\left(1 + \frac{\sqrt{p_\alpha^2 + p_\beta^2}}{2}\right)} \tag{7}$$

In order to obtain the apparent inductances, the integration of the incremental in terms of RMS phase current must be implemented. The estimated apparent inductances are stored in a look-up table corresponding to every RMS phase current at the resolution of 0.1 A in this study and updated every PWM cycle [16].

TABLE II
CALCULATION OF *g*

Voltage vectors	*g*
V_1 and V_2	$\frac{3}{\frac{di_A^{(1)}}{dt} - \frac{di_A^{(0)}}{dt} + \frac{di_B^{(2)}}{dt} - \frac{di_B^{(0)}}{dt}}$
V_2 and V_3	$\frac{3}{\frac{di_A^{(2)}}{dt} - \frac{di_A^{(0)}}{dt} + \frac{di_B^{(3)}}{dt} - \frac{di_B^{(0)}}{dt}}$
V_3 and V_4	$\frac{-3}{\frac{di_A^{(4)}}{dt} - \frac{di_A^{(0)}}{dt} + \frac{di_C^{(3)}}{dt} - \frac{di_C^{(0)}}{dt}}$
V_4 and V_5	$\frac{-3}{\frac{di_A^{(4)}}{dt} - \frac{di_A^{(0)}}{dt} + \frac{di_B^{(5)}}{dt} - \frac{di_B^{(0)}}{dt}}$
V_5 and V_6	$\frac{-3}{\frac{di_A^{(5)}}{dt} - \frac{di_A^{(0)}}{dt} + \frac{di_B^{(6)}}{dt} - \frac{di_B^{(0)}}{dt}}$
V_6 and V_1	$\frac{3}{\frac{di_A^{(1)}}{dt} - \frac{di_A^{(0)}}{dt} + \frac{di_C^{(6)}}{dt} - \frac{di_C^{(0)}}{dt}}$

C. Estimation of stator resistance and permanent magnet flux linkage

The dynamic model of the IPMSM for parameter estimation is described in the synchronous reference frame as followed:

$$\hat{V}_d = \hat{R}_s i_d + \hat{L}_d \frac{di_d}{dt} - \hat{\omega}_{re} \hat{L}_q i_q$$

$$\hat{V}_q = \hat{R}_s i_q + \hat{L}_q \frac{di_q}{dt} + \hat{\omega}_{re}(\hat{L}_d i_d + \hat{\lambda}_f) \tag{8}$$

where $\hat{V}_d$ and $\hat{V}_q$ are the estimated the stator voltage; i_d and i_q are the stator currents; $\hat{\omega}_{re}$ is the estimated electrical rotor speed; $\hat{R}_s$ is the estimated stator resistance; $\hat{\lambda}_f$ is the estimated permanent magnet flux linkage; $\hat{L}_d$ and $\hat{L}_q$ are the estimated inductances, which are updated every PWM cycle.

The RLS algorithm for estimating R_s and λ_f is described by equations (9):

$$\theta_{est(k)} = \theta_{est(k-1)} + K_{(k)} \varepsilon_{(k)}$$

$$\varepsilon_{(k)} = y_{(k)} - \varphi_{(k)}^T \theta_{est(k-1)}$$

$$K_{(k)} = P_{(k-1)} . \varphi_{(k)} . [\lambda . I - \varphi_{(k)}^T . P_{(k-1)} . \varphi_{(k)}]$$

$$P_{(k-1)} = [I - K_{(k)} . \varphi_{(k)}^T] . P_{(k-1)} / \lambda \tag{9}$$

where y is the output matrix, θ_{est} is the estimated parameter vector, φ is the feedback matrix, λ is the forgetting factor, I is the identity matrix, ε is the estimation error, and K and $P_{(k)}$ are correction gain matrices.

$$y = \begin{bmatrix} \hat{V}_d + \hat{\omega}_{re} \hat{L}_q i_q \\ \hat{V}_q - \hat{\omega}_{re} \hat{L}_d i_d \end{bmatrix}; \varphi_{(k)}^T = \begin{bmatrix} i_d & 0 \\ i_q & \omega_{re} \end{bmatrix}; \theta_{est} = \begin{bmatrix} \hat{R}_s \\ \hat{\lambda}_f \end{bmatrix} \tag{10}$$

The sampling frequency of the recursive least square algorithm is the same as the switching frequency, which is also the sampling frequency of the control system.

III. Experimental Setup

Fig. 1 shows the experimental setup for sensorless direct torque and flux control of an IPMSM. The tested machine is the commercial Kollmorgan IPMSM, of which the parameters are shown in Table III. The DC machine is coupled with the tested IPMSM for loading. An H-bridge is connected to the DC machine for varying the load current. DS1103 is used to implement the control scheme, the estimation of rotor speed, position and the identification of all four machine parameters. The phase currents of the machine are sensed by using the Anisotropic Magnetoresistance (AMR) current sensors with bandwidth up to 2 MHz. The currents transducers are connected to the analog input of DS1103 for current feedback of the control system. At the same time the sensed currents are sampled by three channels 16 bits Analog to Digital Converter (ADC FM164) which is plugged in the High Pin Count (HPC) of the Field-programmable gate array (FPGA). FPGA is used to generate the PWM signal for the SiC Inverter and calculate the current derivatives based on the sampled currents. FPGA communicates with DS1103 via digital input and output signals.

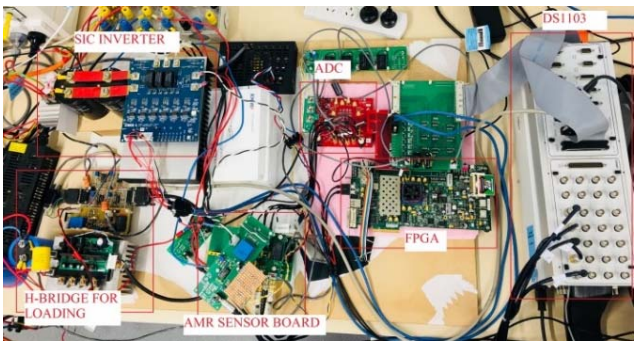

Fig.1. The setup for experiment.

TABLE III
PARAMETERS OF THE TESTED IPMSMS

Number of pole pair	2
Stator resistance	5.8 Ω
Permanent magnet flux linkage	0.533 Wb
d-axis inductance	44.8 mH
q-axis inductance	102.7 mH
Phase voltage	230 V
Phase current	3 A
Rated torque	6 Nm
Rated speed	1500 rpm

The block diagram of the sensorless direct torque and flux control system is presented in Fig. 2. The rotor speed, position and machine parameters are estimated in DS1103 based on the current derivatives received from FPGA, *d*- and *q*- currents, and the estimated *d*- and *q*- voltage. The estimated machine parameters are then used to estimate machine torque and flux for the feedback of the torque and flux control loop, respectively.

The estimated torque and flux are expressed as followed:

$$\lambda_{ds} = \hat{L}_d i_{ds} + \hat{\lambda}_f \tag{11}$$

$$\lambda_{qs} = \hat{L}_q i_{qs}$$

$$\hat{\lambda} = \sqrt{\lambda_{ds}^2 + \lambda_{qs}^2}$$

$$\hat{T} = \frac{3P}{2}\left[\hat{\lambda}_f i_{qs} + \left(\hat{L}_d - \hat{L}_q\right) i_{ds} i_{qs}\right] \tag{12}$$

IV. SIMULATION AND EXPERIMENTAL RESULTS

A. Simulation results

The *d*- and *q*- axis inductances of the tested IPMSM were first measured by using the off-line standstill test as shown in [17]. The off-line measured machine inductances are shown in Fig. 3. It is noted that when the operating current varies from 0.1A to 3 A (rated value), L_d is almost unchange, however, L_q decreases from about 0.13 H to about 0.102 H due to the saturation of the magnetic.

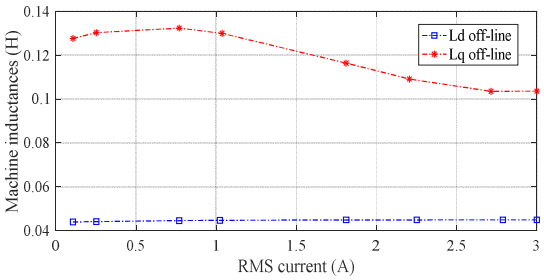

Fig. 3. Machine inductances identified by off-line method.

The proposed sensorless direct torque an flux control system was simulated in Matlab-Simulink. The values of off-line measured inductances (*Ld off-line* and *Lq off-line*) corresponding to the operating RMS phase current, which are fitted by the polynomial curves as shown in (13) and (14) are set in the IPMSM simulation model as the *Ld ref* and *Lq ref*, respectively.

$$Ld\ offline = 0.096 I_{rms}^3 - 0.654 I_{rms}^2 + 1.469 I_{rms} + 43.775 \tag{13}$$

$$Lq\ offline = 5.268 I_{rms}^3 - 27.325 I_{rms}^2 + 27.439 I_{rms} + 124.95 \tag{14}$$

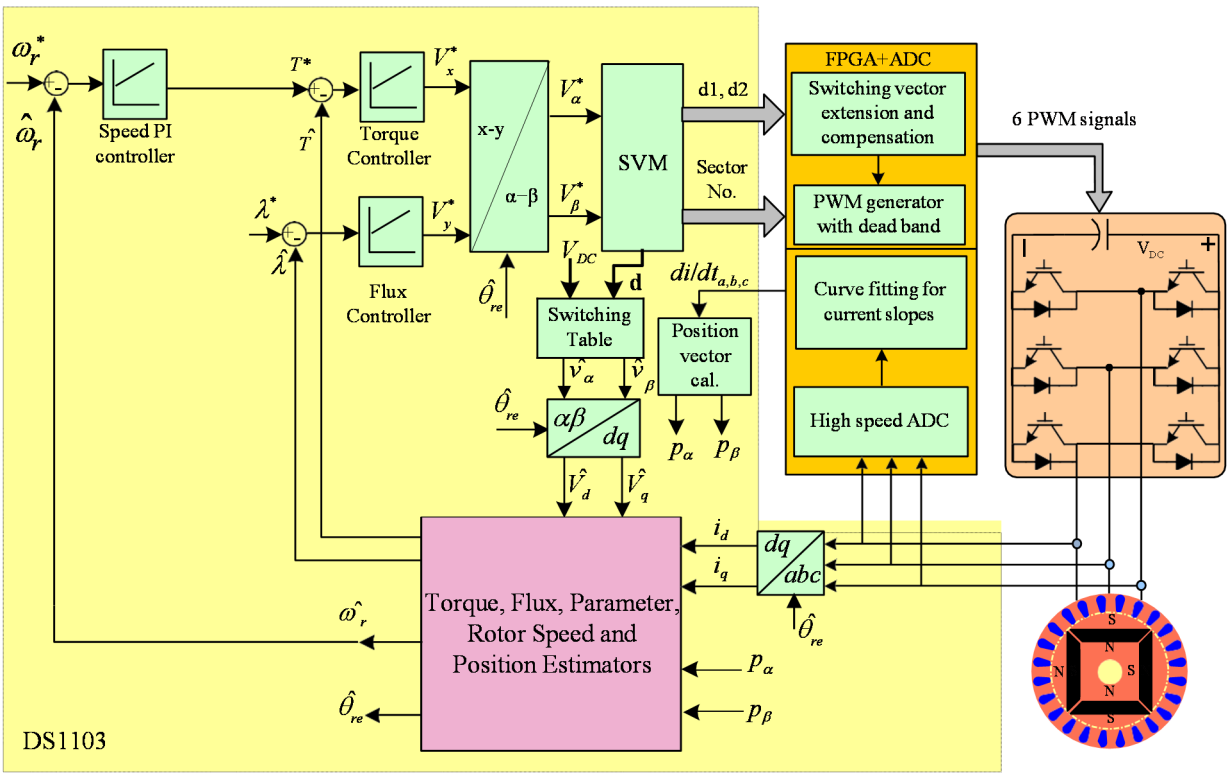

Fig. 2. The block diagram of the sensorless direct torque and flux control system.

Fig. 4 shows the estimation of machine inductances during the speed acceleration from 0 rpm to 1450 rpm under no load condition. The first plot of Fig. 4 shows the operating RMS of the phase current, while the second plot presents the operating speed. The third and the fourth plots of this figure display the estimated inductances (*Ld est* and *Lq est*) and the setting inductances of IPMSM model (*Ld ref* and *Lq ref*), respectively.

In order to evaluate the accuracy of the inductance estimation, the estimated and setting inductances corresponding to the phase RMS current during the speed acceleration are shown in Fig. 5. It is clear that the estimated *Ld est* and *Lq est* are matched closely with the setting *Ld ref* and *Lq ref* of the IPMSM model, respectively.

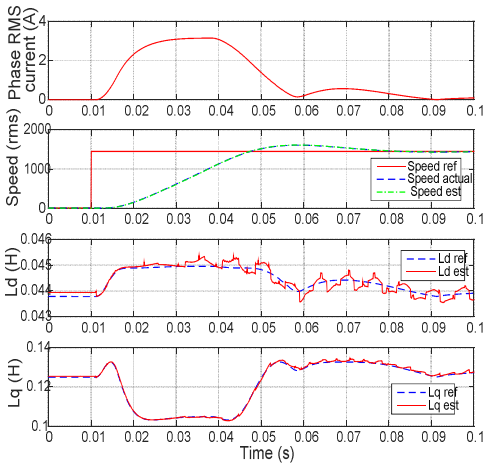

Fig. 4. Estimation of machine inductanes during the speed acceleration from 0 to 1450 rpm under no load condition (simulation).

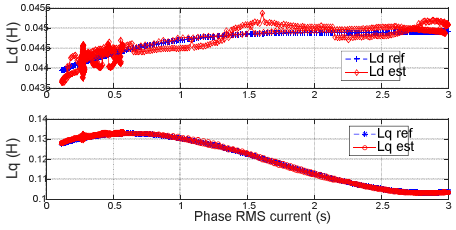

Fig. 5. Estimation of machine inductances versus phase RMS current during the speed acceleration from 0 to 1450 rpm under no load condition (simulation).

Fig. 6 shows the estimation of torque, flux and rotor position of the proposed method when the machine accelerate from 0 to 1450 rpm under no load condition. The first plot shows the actual torque (*Torque actual*), torque estimated by using nominal values of machine parameters as shown in table III (*Torque normal*) and the estimated torque by the proposed method obtained according to (12) (*Torque proposed*). The second plot presents the actual flux (*Flux actual*), the flux estimated by using the nominal values of machine parameters (*Flux normal*) and estimated flux by the proposed method using (11) (*Flux propsed)*. It is obvious that the estimated torque and flux by the proposed method match more closely to the actual ones than the estimated torque and flux using the nominal parameter values during the steady and transient operation, especially during the transient state when there is a signifcant variation of *q*- axis inductances. The third and fourth plots of Fig. 6 display the operating speed and the position estimation error, respectively. The position estimation error is within 3 electrical degree during the steady and transient operation, while the speed estimation error is within 12 rpm during the transient state and within 5 rpm during the steady state..

Stator resistance and the permanent magnet flux linkage are estimated during the steady operating state of the control system. The estimation results of all four parameters of the machine when running at 1000 rpm under full load condition are presented in Fig. 7. It is clear that the estimation errors between the estimated and the setting inductances are about 1 mH and that the estimated stator resistance and permanent magnet flux linkage track very well with the setting values of the IPMSM model, which are 5.8 Ω and 0.533 Wb, respectively.

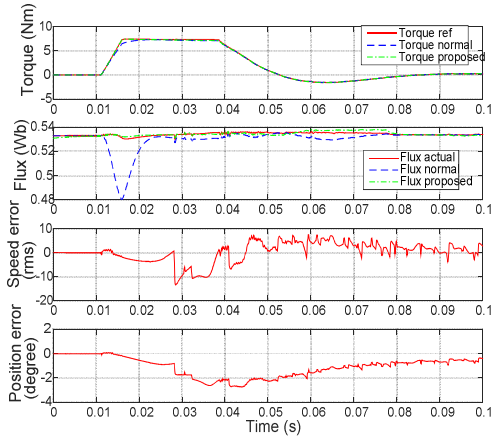

Fig. 6. Estimation of machine torque, flux, speed and position during the speed acceleration from 0 to 1450 rpm under no load condition (simulation).

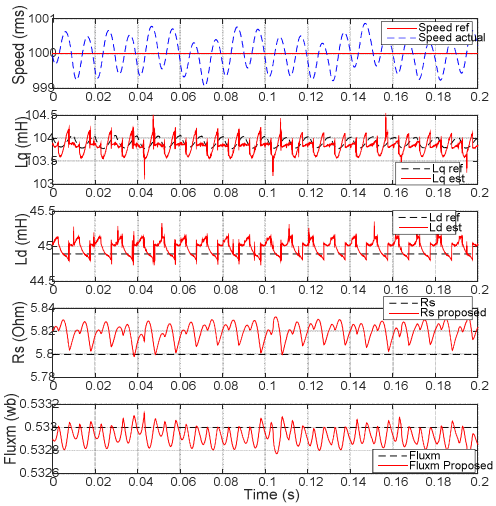

Fig. 7. Estimation of all four parameters at the speed of 1000 rpm under full load condition (simulation).

B. Experimental results

Fig. 8 shows the estimation of machine inductances when the machine accelerate from 0 to 900 rpm. At the time 1.02 s, the machine starts accelerating, the RMS current ubruptly increases from 0.9A to 2.6A. The estimated L_q drops ubruptly from about 138 mH to 110mH, while the estimated L_d remains almost unchanged. When the speed reaches the stable state, the RMS current recovers to nearly 1 A and the L_q returns to about 137mH. It is obvious that, the estimated inductances track very fast with the variation of the actual values.

Fig. 9 compares the estimation of L_d and L_q by the proposed method and the off-line method shown in [17] when the machine operates stably at 900 rpm under different load levels from no load to 120% of rated torque. It is clear that the on-line estimated inductances closely match the off-line measured ones. The deviation of the on-line estimated and the off-line measured value are very small compared to the nominal values of 102.7mH and 44.2mH for L_q and L_d, respectively.

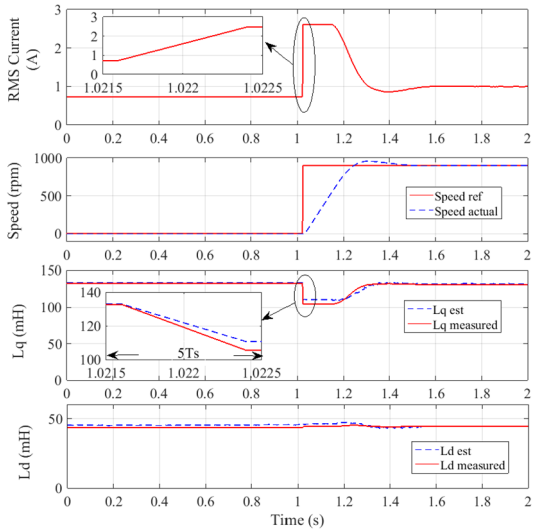

Fig. 8. Estimated inductances versus RMS current during the acceleration from zero to 900 rpm (experiment).

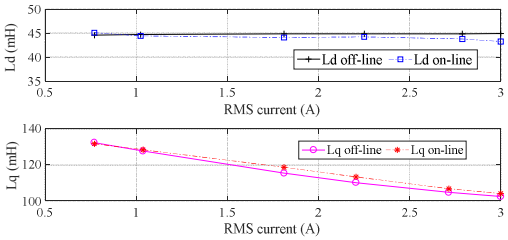

Fig. 9. Estimated inductances at 900 rpm under different current levels (experiment).

V. Conclusion

This paper has presented an improved sensorless direct torque and flux control technique for an IPMSM drive system. The current derivatives at one zero- and two active-voltage vectors during every PWM cycles are measured to estimate rotor speed, position and machine inductances. The stator resistance and permanent magnet flux linkage are identified on-line by using the recursive least square method. The simulation results have shown that all four parameters of the IPMSM including stator resistance, *d*- and *q*- axis inductances, and permanent magnet flux linkage are estimated with high accuracy. The simulation results also demonstrate the improvement of torque and flux estimation during steady and transient state operation as the consequence of using accurate update of machine inductances and permanent magnet flux linkage. The experimental results have shown the fast update of machine inductances and the similar accuracy as the off-line standstill method.

Acknowledgement

This work was supported by Nafosted Vietnam.

Reference

[1] M. F. Rahman, L. Zhong, and K. W. Lim, "A direct torque-controlled interior permanent magnet synchronous motor drive incorporating field weakening," *IEEE Transactions on Industry Applications,* vol. 34, pp. 1246-1253, Nov-Dec 1998.

[2] G. Foo and M. F. Rahman, "A Novel Speed Sensorless Direct Torque and Flux Controlled Interior Permanent Magnet Synchronous Motor Drive," *2008 IEEE Power Electronics Specialists Conference, Vols 1-10,* pp. 50-56, 2008.

[3] Z. Xu and M. F. Rahman, "An Adaptive Sliding Stator Flux Observer for a Direct-Torque-Controlled IPM Synchronous Motor Drive," *IEEE Transactions on Industrial Electronics,* vol. 54, pp. 2398-2406, 2007.

[4] T. F. Chan, W. Wang, P. Borsje, Y. K. Wong, and S. L. Ho, "Sensorless permanent-magnet synchronous motor drive using a reduced-order rotor flux observer," *IET Electric Power Applications,* vol. 2, pp. 88-98, 2008.

[5] C. Yu, J. Tamura, D. D. Reigosa, and R. D. Lorenz, "Position Self-Sensing Evaluation of a FI-IPMSM Based on High-Frequency Signal Injection Methods," *IEEE Transactions on Industry Applications,* vol. 49, pp. 880-888, 2013.

[6] G. Foo and M. F. Rahman, "Sensorless Sliding-Mode MTPA Control of an IPM Synchronous Motor Drive Using a Sliding-Mode Observer and HF Signal Injection," *IEEE Transactions on Industrial Electronics,* vol. 57, pp. 1270-1278, 2010.

[7] C. Silva, G. M. Asher, and M. Sumner, "Hybrid rotor position observer for wide speed-range sensorless PM motor drives including zero speed," *IEEE Transactions on Industrial Electronics,* vol. 53, pp. 373-378, Apr 2006.

[8] Q. Gao, G. M. Asher, M. Sumner, and P. Makys, "Position Estimation of AC Machines Over a Wide Frequency Range Based on Space Vector PWM Excitation," *IEEE Transactions on Industry Applications,* vol. 43, pp. 1001-1011, 2007.

[9] M. X. Bui, D. Guan, D. Xiao, and M. F. Rahman, "A Modified Sensorless Control Scheme for Interior Permanent Magnet Synchronous Motor Over Zero to Rated Speed Range Using Current Derivative Measurements," *IEEE Transactions on Industrial Electronics,* vol. 66, pp. 102-113, 2019.

[10] M. X. Bui, M. F. Rahman, and D. Xiao, "A Hybrid Sensorless Controller of an Interior Permanent Magnet Synchronous Machine Using Current Derivative Measurements and a Sliding Mode Observer," *IEEE Transactions on Industry Applications,* vol. 56, pp. 314-324, 2020.

[11] "IEEE Standard Procedures for Obtaining Synchronous Machine Parameters by Standstill Frequency Response Testing (Supplement to ANSI/IEEE Std 115-1983, IEEE Guide: Test Procedures for Synchronous Machines)," *IEEE Std 115A-1987,* p. 0_1, 1987.

[12] IEC60034-4, "Rotating Electrical Machines Part 4: Methods for Determining Synchronous Machine Quantities From Tests," ed, 2008.

[13] M. S. Rafaq, F. Mwasilu, J. Kim, H. H. Choi, and J. W. Jung, "Online Parameter Identification for Model-Based Sensorless Control of Interior Permanent Magnet Synchronous Machine," *IEEE Transactions on Power Electronics,* vol. 32, pp. 4631-4643, 2017.

[14] S. Ichikawa, M. Tomita, S. Doki, and S. Okuma, "Sensorless control of permanent-magnet synchronous motors using online parameter identification based on system identification theory," *IEEE Transactions on Industrial Electronics,* vol. 53, pp. 363-372, 2006.

[15] K. Liu, Q. Zhang, J. Chen, Z. Q. Zhu, and J. Zhang, "Online Multiparameter Estimation of Nonsalient-Pole PM Synchronous Machines With Temperature Variation Tracking," *IEEE Transactions on Industrial Electronics,* vol. 58, pp. 1776-1788, 2011.

[16] M. X. Bui, M. F. Rahman, D. Guan, and D. Xiao, "A New and Fast Method for On-line Estimation of d and q Axes Inductances of Interior Permanent Magnet Synchronous Machines Using Measurements of Current Derivatives and Inverter DC-Bus Voltage," *IEEE Transactions on Industrial Electronics,* vol. 66, pp. 7488-7497, 2019.

[17] R. Dutta and M. F. Rahman, "A comparative analysis of two test methods of measuring d- and q-axes inductances of interior permanent-magnet machine," *IEEE Transactions on Magnetics,* vol. 42, pp. 3712-3718, Nov 2006.